TASK QUARTERLY 5 No 4 (2001), 567–577

3D INVISCID FLUTTER OF ROTOR BLADES AND STATOR/ROTOR STAGE

ROMUALD RZĄDKOWSKI[1,2] AND VITALY GNESIN[3]

[1]*Institute of Fluid-Flow Machinery,*
Polish Academy of Sciences,
Fiszera 14, 80-952 Gdansk, Poland

[2]*Polish Naval Academy,*
Śmidowicza 69, 81-103 Gdynia, Poland
z3@imp.gda.pl

[3]*Department of Aerohydromechanics,*
Institute for Problems in Machinery,
Ukrainian National Academy of Sciences,
2/10 Pozharsky, 310046 Kharkov, Ukraine
gnesin@ipmach.kharkov.ua

(Received 28 June 2001; revised manuscript received 12 August 2001)

Abstract: Numerical calculations of the 3D transonic flow of an ideal gas through turbomachinery rotor blade row and stator, rotor blades moving relatively one to another with taking into account the blades oscillations are presented.

The approach is based on the solution of the coupled aerodynamic-structure problem for the 3D flow through the turbine stage in which fluid and dynamic equations are integrated simultaneously in time.

An ideal gas flow through the mutually moving stator and rotor blades with periodicity on the whole annulus is described by the unsteady Euler conservation equations, which are integrated using the explicit monotonous finite-volume difference scheme of Godunov-Kolgan and moving hybrid H-H grid.

The structure analysis uses the modal approach and 3D finite element model of a blade. There has been performed the calculation for the last stage of the steam turbine with rotor blades of 0.765 m.

Keywords: flutter, blades, unsteady forces

1. Introduction

The cascade flutter is characterised by aerodynamic interaction among oscillating blades in the blade row. Its importance can be understood from the fact that the unsteady aerodynamic force on blades is heavily dependent on the interblade phase angle. From this standpoint neighbouring blade rows, *e.g.*, a neighbouring rotor or stator or contra-rotating fan cascade, will also have a considerable influence on the unsteady aerodynamic force because blade rows are closely placed in actual turbomachines.

A literature survey on flutter prediction methods is beyond the scope of this paper and the interested reader should consult (Marshal and Imregun [1]). However, a brief overview will be given here for the sake of completeness.

Most flutter computations consider a typical sector vibrating in some given assembly mode (or interblade phase angle) for which flutter is expected to occur. In other words, the flutter mode must be known before the analysis, though it is also possible to consider the individual stability of each mode in turn. In such, usually linear analysis, the interblade phase angle must be prescribed at the periodic boundaries.

In recent times the new approaches based on the simultaneous integration in time of the equations of motion for the structure and the fluid are developed (Bakhle *et al.* [2], He [3]; Moyround *et al.* [4], Rządkowski [5], Rządkowski and Gnesin [6, 7], He and Ning [8], Bendiksen [9], Gnesin *et al.* [10–12], Carstens and Belz [13]). These approaches are very attractive due to the correct formulation of a coupled problem, as the interblade phase angle at which a stability (instability) would occur is part of the solution. Generally, the papers presented above take into consideration only the rotor blades. The stator blades are modeled by the interblade phase angle of the rotor blades as the initial condition.

Hall and Silkowski [14] can be cited as one of a few papers investigating into the effect of neighbouring blade rows. They presented an analysis based on two-dimensional multiple blade rows, in which blades of one blade row are oscillating, and showed a remarkable difference of the aerodynamic damping from that of an isolated blade row.

Namba and Ishikawa [15] gives an analytical study on contra-rotating annular cascades with oscillating blades. In that paper the case of blade oscillation of one of the pair cascades but also the case of blade oscillation of both cascades is considered. The analytical method is an extension of one of the authors' unsteady linearized lifting surface theories for a rotating annular cascade [15] to the model of a pair of contra-rotating cascades. Recently the validity of the original code has been confirmed from comparison of the Namba's data with those computed by Schulten's code [16], both of which were submitted to the Third Computational Aeroacoustics Workshop on Benchmark Problems (November, 1999, Ohio Aerospace Institute) as analytical solutions of Category 4 Fan Stator with Harmonic Excitation by Rotor Wake.

In the present study for the first time the algorithm proposed involves the coupled solution of an aerodynamic problem for turbine stage and the dynamic problem for vibrating blades. The last stage of the steam turbine with rotor blades of 0.765 m were used. The numerical results for unsteady aerodynamic forces for the isolated rotor blades and due to stator/rotor interaction are presented.

2. Aerodynamic model

The 3D transonic flow of an ideal gas through a space multipassage blade row is considered. In general the flow is assumed to be aperiodic function from blade to blade (in pitchwise direction), so the calculated domain includes all blades of the whole assembly.

The flow equations will be written for a three dimensional Cartesian coordinate system which is fixed to a rotating blade row.

The spatial solution domain is discretized using linear hexahedral elements. The equations of motion are integrated on moving H-H (H-O) – type grid with the use of explicit monotonous second – order accuracy Godunov – Kolgan different scheme (see [11]).

We assume that the unsteady fluctuations in the flow are due to prescribed blade motions, and the flows far upstream and far downstream from the blade row are at most small perturbations of uniform free streams. So the boundary conditions formulation is based on one-dimensional theory of characteristics, where the number of physical boundary conditions depends on the number of characteristics entering the computational domain.

In general, when axial velocity is subsonic, at the inlet boundary initial values for total pressure, total temperature and flow angles are used in terms of the rotating frame of reference, while at the outlet boundary only static pressure has to be imposed. Nonreflecting boundary conditions can be used, *i.e.*, incoming waves (three at inlet, one at the outlet) have to be suppressed, which is accomplished by setting their time derivative to zero. On the blade surface, zero flux is applied across the solid surface (the grid moves with the blade).

3. Structural model

The blade vibration formulation is based on a modal approach of the coupled problem [5, 17]. The dynamic model of the oscillating blade in linearized formulation is governed:

$$\ddot{q}_i(t)+2h_i\dot{q}_i(t)+\omega_i^2 q_i(t)=\lambda_i(t), \tag{1}$$

where ω_i is natural blade frequency, λ_i is the modal forces vector corresponding to the mode shapes, $h_i=2\omega_i\xi_i$, where ξ_i is the i-th modal damping coefficient. The equations of motion (1) can be solved using any standard integration method.

The modal forces λ_i are calculated at each iteration with the use of the instantaneous pressure field.

4. Numerical results

The numerical calculations have been carried out for the long steam turbine cascade. The important properties of the blade disc are as given below: the disk inner radius $r_o=0.27\,\mathrm{m}$, the bladed-disk junction radius $R=0.667\,\mathrm{m}$, the blade length $L=0.765\,\mathrm{m}$. All geometrical parameters of the blade are presented in [5].

The numerical and experimental verification of the numerical code is presented in [6].

The numerical calculations were performed for harmonic oscillations of the blade row according to natural modes with the same amplitude and interblade phase angle (IBPA). The first mode mainly performs the bending oscillations, the second one both bending and torsional oscillations, the third one torsional oscillations, the fourth and fifth modes perform both bending and torsional oscillations. The natural frequencies of the rotating blade are equal to 99 Hz, 160 Hz, 268 Hz, 297 Hz and 398 Hz, respectively [7].

Figure 1 shows the aerodamping coefficient D (averaged over the blade length) versus the interblade phase angle (IBPA) for the 1st natural mode shapes under harmonic oscillations with different excited frequencies. The negative values of D correspond to the transfer of the mean flow energy to the blade (self-excitation), and positive values to the dissipation of an oscillating blade energy to the flow (aerodamping). The values $f=25,\ldots,$ 400 Hz correspond to different excitation frequencies.

The aerodamping coefficient (averaged over the blade length) versus the IBPA for the 2nd, 3rd, 4th and 5th natural mode shapes respectively under harmonic oscillations with different excited frequencies are presented in [7, 12]. It should be pointed out that the

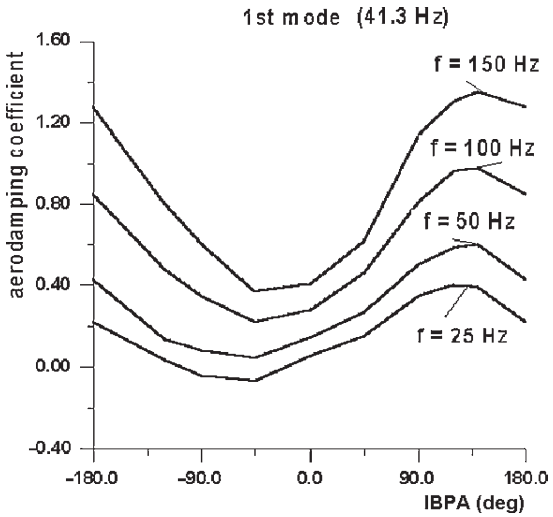

Figure 1. Aerodamping coefficient versus IBPA for the 1st mode and different natural frequencies

oscillations according to the first mode (bending oscillations) are characterised by minimal values of aerodamping coefficient near the IBPA of – 90° (see Figure 1) and transfer the flow energy to the blade (flutter condition) for excitation frequencies $f < 50$Hz. In our case the first natural frequency of rotating blade is $f = 90$Hz and for this mode shapa the blade is stable. The oscillations according to the third mode (torsional oscillations) have the self – excitation area near the IBPA of 90° and for frequencies $f < 300$Hz (see [12]).

All calculations presented in [7, 12] are for the rotor blades for the different interblade phase angle.

In real turbine the interblade phase angle is dependent on the number of stator blades.

The computational results presented below were carried out for the last stage of steam turbine with rotor blades of 0.765m, and the stator to rotor blade number ratio of 56 : 96 (7 : 12).

Numerical calculations have been made using the computational H-grid of 10×24×58 grid points for each stator passage and 10×14×58 grid points for each rotor passage.

One of the important aspects of stator/rotor interaction is the effect of blade response with taking into account the excitation caused by flow ununiformity and excitation due to blades oscillations.

In accordance with the stator/rotor ratio of blades ($z_s : z_r = 7 : 12$) we observe that the load phase lag for i–th blade comparatively to the first one is of $2\pi(i-1)z_s : z_r$ or $7/6\pi(i-1)$.

The blade oscillations are defined with taking into account the first ten natural mode shapes, with taking into account the rotation of the blades. The modal damping coefficients were assumed [5]: $\xi_1 = 0.00075$, $\xi_2 = 0.00094$, $\xi_3 = 0.0011$, $\xi_3 = \xi_4 = \ldots = \xi_{10}$.

The unsteady modal forces were calculated only for four rotations of rotor blades. The one rotation takes 130 hours of PC CPU time.

The unsteady modal force change includes high frequency harmonic ($\nu = z_s \cdot 50 =$ 2800Hz) corresponding to rotor moving past one stator blade pitch and spectrum of low

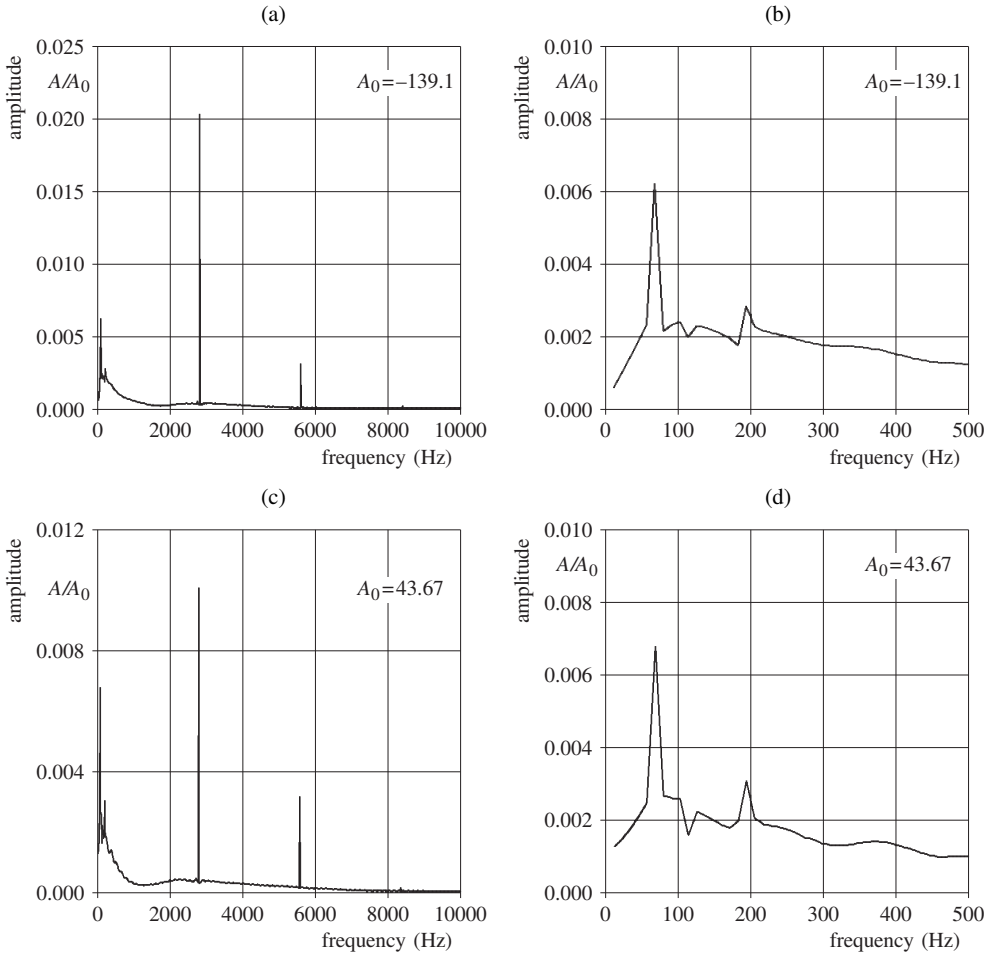

Figure 2. Amplitude-frequency characteristics for unsteady aerodynamical forces: (a), (b) 1st mode; (c), (d) 2nd mode

frequencies (see Figure 2). We are using here the term the 'unsteady modal force', which is equal along the blade length and corresponding to the particular mode shape. This is disadvantage of the modal superposition calculations, where modal force averaged along the length of the blades is calculated.

Figures 2a and 2b present the modal components of the unsteady modal force corresponding to the first mode. It is seen that the high frequency excitations appeared for 2800 Hz (equal to 2% of the steady force $A_0 = 139.1$ N/kg) and for $2 \cdot 2800$ Hz (equal to 0.3% of A_0). The low frequency excitation is 0.62% of A_0 for frequency 73 Hz (see Figure 2b).

Figures 2c and 2d present the modal components of the unsteady modal force corresponding to the second mode. It is seen that the high frequency excitations appeared for 2800 Hz (equal to 1% of the steady force $A_0 = 43.67$ N/kg) and for $2 \cdot 2800$ Hz (equal to 0.3% of A_0). The low frequency excitation is 0.69% of A_0 for frequency 73 Hz (see Figure 2b).

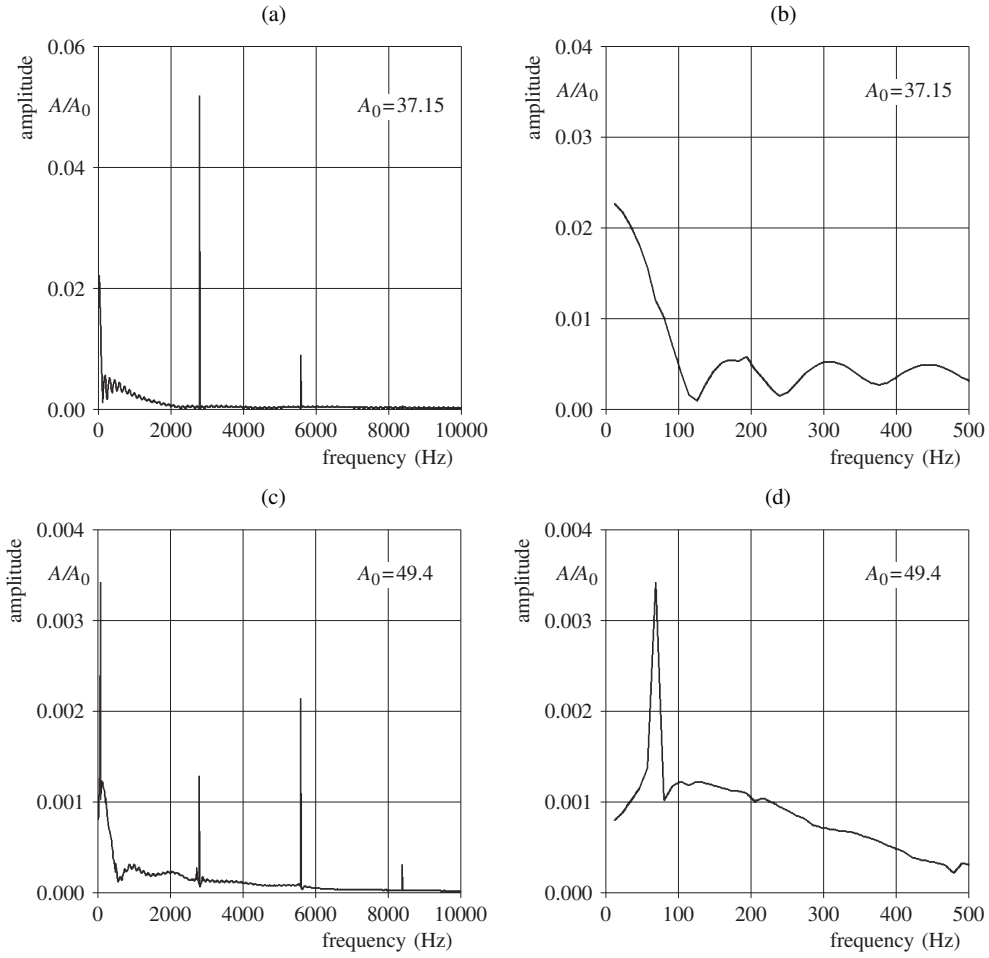

Figure 3. Amplitude-frequency characteristics for unsteady aerodynamical forces: (a), (b) 3rd mode; (c), (d) 4th mode

Figures 3a and 3b present the modal components of the unsteady modal force corresponding to the third mode. It is seen that the high frequency excitations appeared for 2800 Hz (equal to 5% of the steady force $A_0 = 37.15$ N/kg) and for $2 \cdot 2800$ Hz (equal to 1% of $A_0 = 37.15$ N/kg).

Figures 3c and 3d present the modal components of the unsteady modal force corresponding to the fourth mode. It is seen that the high frequency excitations appeared for 2800 Hz (equal to 0.2% of the steady force $A_0 = 49.4$ N/kg) and for $2 \cdot 2800$ Hz (equal to 0.05% of A_0). The low frequency excitation is 0.35% of A_0 for frequency 73 Hz (see Figure 3d). In this case the values of the low frequency excitation are higher than the value of the high frequency excitation.

Figures 4 present the modal unsteady components corresponding to the 6th, 8th and 10th modes. The influence of these modes on the values of the total unsteady modal force is smaller than in the previous cases.

The values of the unsteady forces calculated for the rotating and non-vibrating blades along the blade length are presented in Table 1.

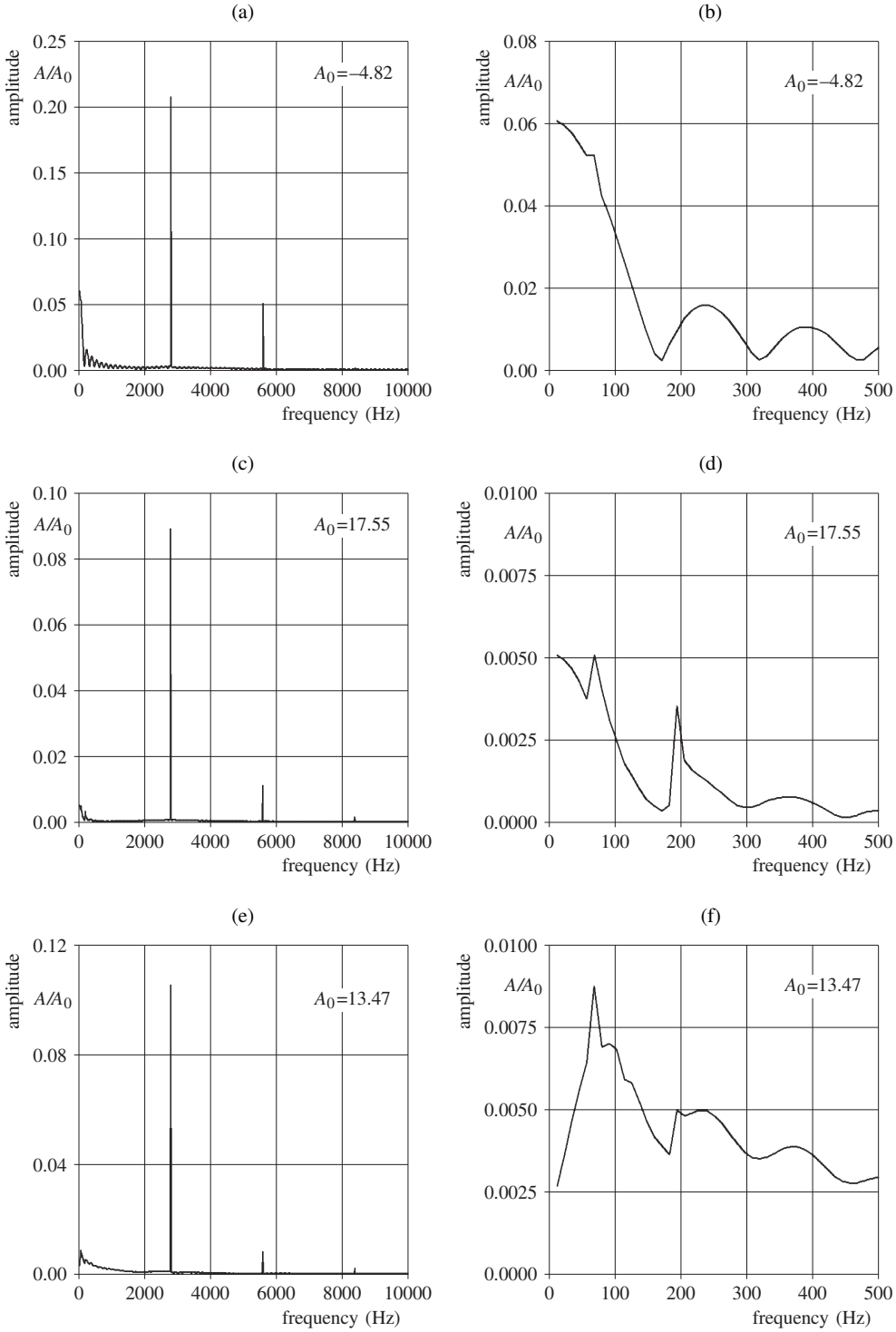

Figure 4. Amplitude-frequency characteristics for unsteady aerodynamical forces: (a), (b) 6^{th} mode; (c), (d) 8^{th} mode; (e), (f) 10^{th} mode

Table 1. The first harmonic components of the unsteady forced along the blade length

Non-vibrating	F_y [%]	F_z [%]	M [%]
the peripheral layer	6	4	7
the middle layer	8	3	29
the root layer	39	59	115
Vibrating	F_y [%]	F_z [%]	M [%]
the peripheral layer	7.8	5.4	6
the middle layer	8.2	3	29
the root layer	39	59	115

The blade motion in the form of the modal coefficients variation in time for the 1st blade is presented in Figures 5, 6. The modal coefficients corresponding to the 1st, 2nd, 3rd and 4th mode shape have been shown in Figure 5. The modal coefficients corresponding to the 6th, 8th, 10th mode shape have been shown in Figure 6.

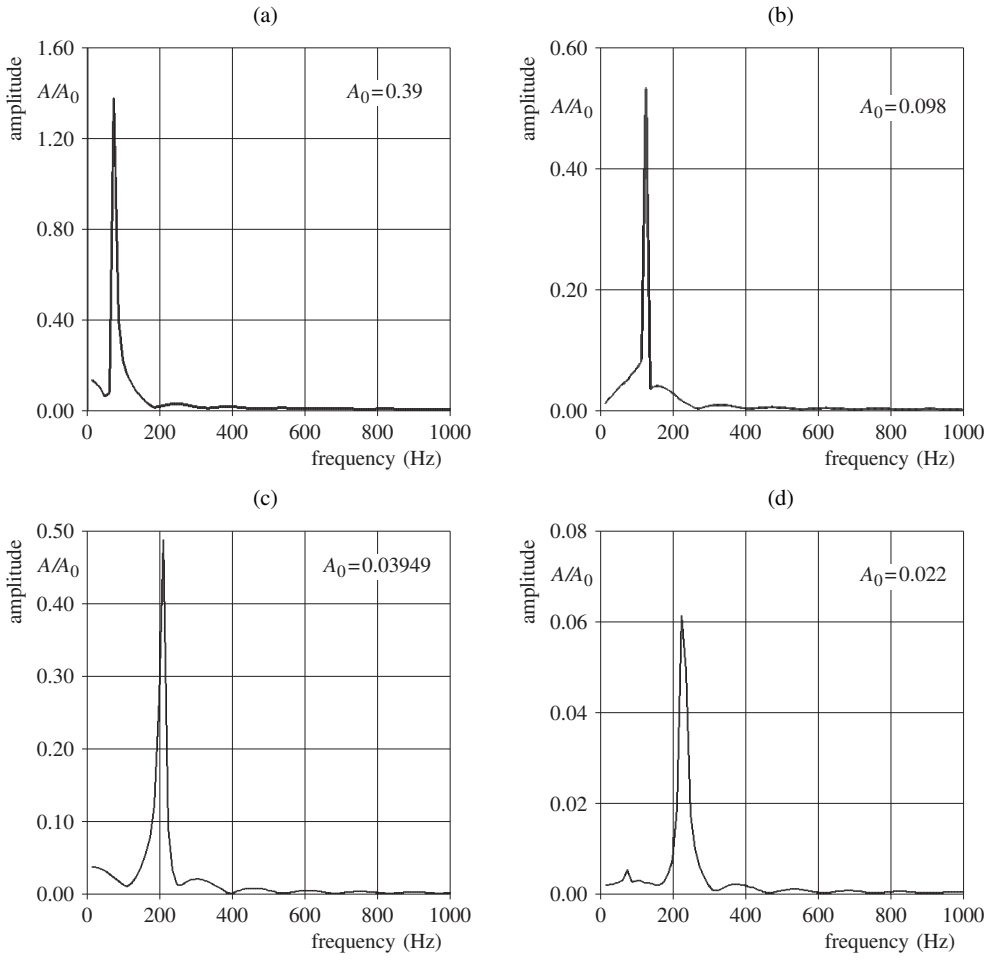

Figure 5. Amplitude-frequency characteristics for blade moving:
(a) 1st mode; (b) 2nd mode; (c) 3rd mode; (d) 4th mode

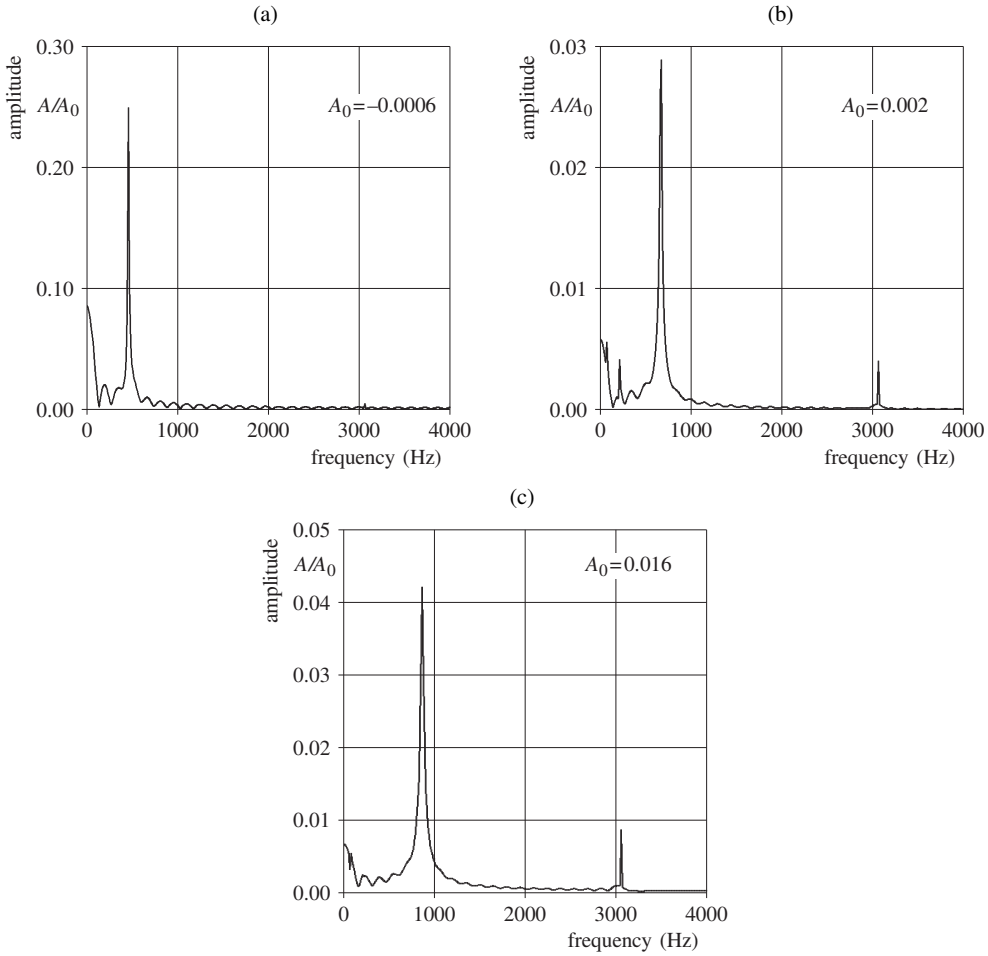

Figure 6. Amplitude-frequency characteristics for blade moving: (a) 6th mode; (b) 8th mode; (c) 10th mode

The unsteady amplitude of the first mode (see Figure 5a) is 1.4 of the steady amplitude $A_0 = 0.39$mm and has frequency 73Hz (99Hz the natural frequency). The unsteady amplitude of the second mode (see Figure 5b) is 0.55 of the steady amplitude $A_0 = 0.098$mm and has frequency 117Hz (160Hz the natural frequency). The unsteady amplitude of the third mode (see Figure 5c) is 0.49 of the steady amplitude $A_0 = 0.039$mm and has frequency 188Hz (268Hz the natural frequency). The unsteady amplitude of the fourth mode (see Figure 5d) is 0.061 of the steady amplitude $A_0 = 0.022$mm and has frequency 214Hz (297Hz the natural frequency).

The unsteady amplitude of the sixth mode (see Figure 6a) is 0.25 of the steady amplitude $A_0 = 0.0006$mm and has frequency 375Hz (598Hz the natural frequency). The unsteady amplitude of the eight mode (see Figure 6b) is 0.029 of the steady amplitude $A_0 = 0.002$mm and has frequency 600Hz (863Hz the natural frequency). The unsteady amplitude of the tenth mode (see Figure 6c) is 0.042 of the steady amplitude $A_0 = 0.0016$mm and has frequency 750Hz (1124Hz the natural frequency).

The first three modes bring their contribution into the blade motion. The vibration blade frequencies for different modes in the gas flow is about 30% less than their natural frequencies (see Figures 5 and 6).

5. Conclusions

A partially-integrated method based on the solution of the coupled aerodynamic-structure problem is adopted for unsteady 3D flow through a turbine stage with taking into account the rotor blades oscillations.

The paper has investigated the mutual influence of both outer nonuniform flow and blades oscillations. The interblade phase angle of blades oscillations depends not only on unsteady forces lag but on the blade natural frequencies, as well.

It has been shown that amplitude-frequency spectrum includes the harmonics with frequencies which are not multiple to the rotation frequency.

All calculations were done for only four rotations of the rotor. The higher number of rotations must be taken into consideration. Presented results show the possibility of appearance of the low frequency vibration in the case of mistuning of the rotor, stator blades and any nonuniformity of the inlet or the exit flow.

Acknowledgements

The authors wish to acknowledge KBN for the financial suport of this work (project 7 T07B 010 16).

All numerical calculations were made at the Academic Computer Center TASK (Gdansk, Poland).

References

[1] Marshall J G and Imregun M 1996 *Journal of Fluids and Structures* **10** 237
[2] Bakhle M A, Reddy T S R and Keith T G 1992 *AIAA Journal* **30** (1) 163
[3] He L 1984 *Journal of Computational Fluid Dynamics* **3** 217
[4] Moyroud F, Jacquet-Richardet G and Fransson T H 1996 *A Modal Coupling for Fluid and Structure Analysis of turbomachines Flutter. Application to a Fan Stage* ASME Paper 96-GT-335 1–19
[5] Rządkowski R 1998 *Dynamics of Steam Turbine Blading, Part Two Bladed Discs* Ossolineum Wrocław-Warszawa
[6] Rządkowski R and Gnesin V 2000 *The Numerical and Experimental Verification of the 3D Inviscid Code* Transaction of the Institute of Fluid-Flow Machinery **106** 69
[7] Rządkowski R and Gnesin V 2001 *Aeroelastic Behaviour of the Last Stage Steam Turbine Blades. Part I. Harmonic Oscillations* Transaction of the Institute of Fluid-Flow Machinery **108** 59
[8] He L and Ning W 1998 *Nonlinear Harmonic Analysis of Unsteady Transonic Inviscid and Viscous Flows* Unsteady Aerodynamics and Aeroelasticity of Turbomachines, Proc. of the 8th International Symposium, September 14–18, Stockholm, Sweden, pp. 183–189
[9] Bendiksen O O 1998 *Nonlinear Blade Vibration and Flutter in Transonic Rotors* Proc. of ISROMAC – 7, The 7^{th} Intern. Symp. on Transport Phenomena and Dynamics of Rotating Machinery, February 22–26, Honolulu, Hawaii, USA
[10] Gnesin V I, Rządkowski R and Kolodyazhnaya L V 2000 *A coupled Fluid-Structure Analysis for 3D Flutter in Turbomachines* ASME Paper 2000-GT-0380
[11] Gnesin V I and Rządkowski R 2000 *The Theoretical Model of 3D Flutter in Subsonic, Transonic and Supersonic Inviscid Flow* Transaction of the Institute of Fluid-Flow Machinery **106** 45
[12] Gnesin V and Rządkowski R 2001 *Aeroelastic Behaviour of the Last Stage Steam Turbine Blades. Part II. Coulped Fluid-Structure Oscillations Harmonic Oscillations* Transaction of the Institute of Fluid-Flow Machinery **108** 73

[13] Carstens V and Belz J 2000 *Numerical Investigation of Nonlinear Fluid-Structure Interaction in Vibrating Compressor Blades* ASME Paper 2000-GT-0381
[14] Hall K C and Silkowski P D 1997 *ASME Journal of Turbomachinery* **119** 85
[15] Namba M and Ishikawa A 1983 *ASME Journal of Engineering for Power* **105** 138
[16] Schulten J B H M 1982 *AIAA Journal* **20** (10) 1352
[17] Bathe K and Wilson E 1976 *Numerical Methods in Finite Element Analysis* Prentice-Hall, Inc Englewood Cliffs, New Jersey